

Design and Evaluation of an Affective, Continuum Robotic Appendage for Child-Robot Interaction

Deanna Kocher, Juliette Bendheim, and Keith E. Green, *Senior Member, IEEE*

Abstract—We introduce a robotic appendage (a “fin”) for a non-humanoid mobile robot that can communicate affect to child collaborators. Affective configurations were generated from a collection of cartoon images that featured characters with floppy or bunny ears. These images were classified according to the six Ekman emotions, analyzed to create ideal emotion configurations, and validated with a user study. From these configurations, we designed multiple continuum robot fin appendages and evaluated them based on (a) their ability to achieve the generated affect configurations, and (b) their durability for sustained use in child-robot interaction studies.

I. INTRODUCTION

Displays of affect and social behaviors can be critical when trying to facilitate communication from a robot to a child [1], [2]. Such communication will vary between robots of different forms. For a humanoid robot like Nao (commonly used in child-robot studies [3], [4]), communication can be mapped directly from human behaviors. For more abstract-looking, non-humanoid robots, communication cannot be mapped in this way; mapping is indirect, and often requires some other referent. While this presents a challenge in designing non-humanoid robots, non-humanoid robots offer advantages in child-robot interaction; namely, increased acceptance [5] and more realistic expectations about what the robot can do [6].

Non-humanoid robots often rely on physical movement to communicate to human collaborators. For our non-humanoid design, these movements come from an appendage situated at the top of the robot that is something of a rabbit-ear. We refer to it, simply, as a “fin” (Fig. 1). This design was selected as it emphasizes curvilinear shapes and movements associated with “positive perceptions” [7] that may help facilitate positive and engaging child-robot interactions. These interactions may, in turn, encourage child-robot collaboration.

To design affective motions for non-humanoid robots, engineers and designers frequently draw on the knowledge of animators. The literature reports on two approaches to this: either animators design for a specific robot behavior [8] or behaviors are derived from a specific cartoon character that is similar to the form factor of the robot [9]. In this paper, we present an alternative method for informing robot behavior by drawing on animation. Rather than drawing on a specific cartoon character or having animators design explicitly for our robot, we take a bottom-up approach where we generate affective configurations from a sizable set of images of different cartoon characters. We assign images to different



Figure 1. The robot’s appendage (or what we call, simply, the “fin”) interacting with a child.

Ekman emotions [10], and derive generalized configurations from the dataset for each emotion. To validate our approach, we conducted a user study on the generalized configurations to confirm that these new configurations are perceived as expected. To achieve these configurations, we explore and evaluate several different continuum [22] designs. Continuum designs were chosen over traditional rigid links as they (a) can achieve diverse configurations with a few degrees of freedom, and (b) are more compliant, making them safer for interactions with children. In this paper, we focus on static configurations (poses) over dynamic movements (gestures) to understand the mechanical constraints of this type of design.

II. RELATED WORK

A. Social Robots for Child-Robot Interaction

Affective displays and social behaviors can have a significant impact on how children perceive robot companions and the affordances they extend to them [11][12]. Young children are often overly animistic, believing that robots have emotional and biological states [13]. Consequently, children engage with robots in a number of different ways, including looking to robots regularly, talking to robots, and physically helping robots [14].

In addition to impacting how children perceive robots and behave with them, social robots can positively impact children’s development and mental states. For autistic children, social robots offer a less daunting way for children to enter into relationships and build social skills than normal human-human social situations [15]. Interacting with a social

Juliette Bendheim was with the Sibley School of Mechanical and Aerospace Engineering, Cornell University, Ithaca NY 14853 USA (jb974@cornell.edu).

Deanna Kocher is with the Sibley School of Mechanical and Aerospace Engineering, Cornell University, Ithaca NY 14853 USA (drk225@cornell.edu).

Keith E. Green, Departments of Design & Environmental Analysis and the Sibley School of Mechanical and Aerospace Engineering, Cornell University, Ithaca NY 14853 USA (keg95@cornell.edu).

robot can also improve children’s positive affect. Introducing a social robot in a hospital increased children’s positive emotions (and decreased negative emotions) more than a digital character or a stuffed animal [16]. Social behaviors can also help maintain children’s attention, though this can be distracting when not related to the task at hand [17].

B. Affective Robots & Animation

Affective displays can help robots communicate appropriately with individuals and even gain empathy from a collaborator. For many robots with humanoid features, human movements and affective displays can be mapped to a robot somewhat directly. For Kismet, this includes facial expressions and head movements [18]; for Nao this focuses on gaze, head movements, and gestures [19]. This mapping holds true even for some non-humanoid robots that have singular human features, such as eyes, where robots can mimic human gaze patterns to create similar responses [20].

While non-humanoid robots cannot directly map movements in this way, many poses and gestures can create affect in non-humanoid robots. Both static and dynamic configurations can achieve this, with static poses suggesting valence and dynamic gesture velocity suggesting arousal [21]. Bretan, Hoffman, & Weinberg [10] demonstrates this in a study of static versus dynamic behaviors of a non-humanoid robot, Shimi. Robot poses and gestures were designed both by-hand and generated by algorithms to fit one of the six Ekman emotions; these poses and gestures were evaluated by the degree to which individuals perceived the poses and gestures as the “correct” emotion. While gestures performed significantly better than poses, both types of stimuli generated above-chance responses for the correct emotion. Similar evaluations have been done with non-humanoid robots such as Gertie [9] and the greeting machine [8]. With five DoF, Gertie was able to achieve joy, sadness, surprise, and fear. While fear and surprise were recognized at above-chance rates, they were often confused with other emotions.

C. Continuum Design

Continuum robots have a few advantages over traditional robots, including adaptivity to different environments and compliance. Continuum robot designs may be a series of underactuated rigid links (hyper-redundant vertebrae) or true continuum designs that can achieve curvature at any location along its length, like octopus tentacles [22]. These designs can be robust and dynamic, achieving configurations that would be difficult to impossible for traditional robot arms. Continuum robots vary in material, scale, and methods of actuation. Vine inspired robots have navigated small spaces for NASA applications [23], while other continuum robots create larger, habitable spaces [24]. Many designs are actuated by tendons [24], but some rely on pneumatics [25] or individually activated panels [26]. Depending on the type of continuum design (hyper-redundant or true continuum) material compositions also differ; true continuum designs typically use softer materials such as silicones and plastics, while hyper-redundant designs might feature rigid sections joined by rigid or elastic components [22]. As presented in Section IV, we explored different continuum designs for our fin based on our analysis of cartoon character behaviors.

III. CARTOON IMAGE ANALYSIS

We compiled a total of 202 images of “bunny ears” and “floppy ears” (floppy dog ears) and analyzed these to define configurations for our fin design (Fig. 2). The ears of these characters were drawn from television and movies of the last half century, and include both 2D and 3D animation styles. We initially collected images from other cartoon animal appendages such as tails, pointy-eared animals, and fish fins; but these did not match the orientation or DoF of our conceptualized “fin”, so we excluded them from our analysis.



Figure 2. Sample cartoon images with ear tracing. ‘Rabbit’ with head angle adjustment and ‘Tramp’ with traced floppy ear.

A. Image Coding

The 202 images were categorized by four student researchers who were independently presented them and asked to assign each image to one of the Ekman emotions: anger, fear, disgust, sadness, happiness, and surprise. Images with at least 75% agreement were selected for further analysis. 75% agreement was achieved by 94 of the 128 bunny ears and 78 of the 89 floppy ears. Twenty-six of these agreed upon images were not analyzed due to part of the ear being cut off, resulting in 69 bunny ears and 62 floppy ears included in our final analysis. Table I shows the emotion distribution of these images. “Disgust” was not included in further analysis due to low image count in this category.

The cartoon ear analysis was completed in AutoCAD by tracing the top and bottom lines of the ears. A center line was then created by connecting segments from the top and bottom lines and also tracing the midpoints of these lines (see the red and blue lines in Fig. 2). To control for individual differences in the images, we completed the following transformations:

TABLE I. PERCENTAGE AND EMOTION BREAKDOWN FOR BUNNY AND FLOPPY EAR CARTOONS

| Type | Emotion | Count | Percent |
|--------|-----------|-------|---------|
| Bunny | Happy | 31 | 21.53 |
| Bunny | Sad | 16 | 11.11 |
| Bunny | Surprised | 12 | 8.33 |
| Bunny | Fear | 7 | 4.86 |
| Bunny | Disgust | 3 | 2.08 |
| Bunny | Anger | 14 | 9.72 |
| Floppy | Happy | 30 | 20.83 |
| Floppy | Sad | 8 | 5.56 |
| Floppy | Surprised | 13 | 8.33 |
| Floppy | Fear | 3 | 2.08 |
| Floppy | Anger | 8 | 5.56 |
| Floppy | Disgust | 0 | 0.00 |

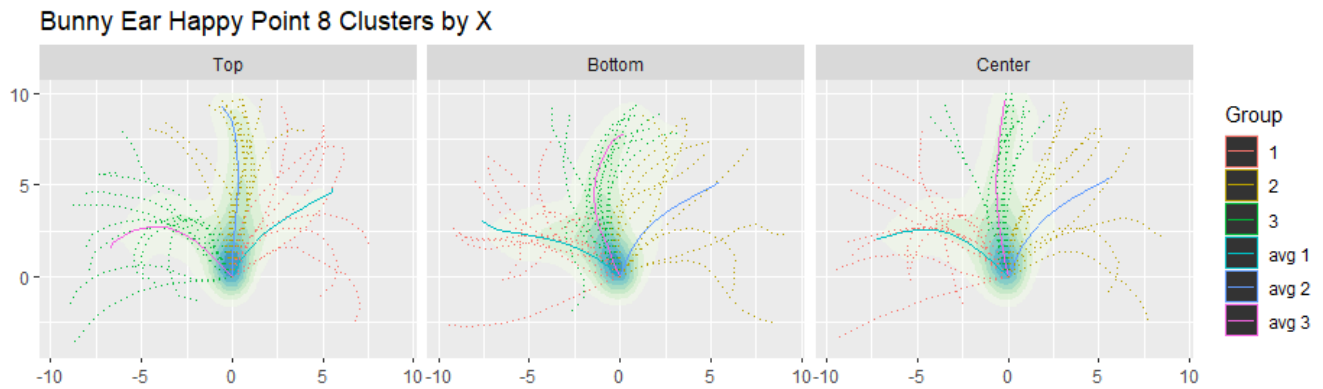


Figure 3. 2D density plots for the top, bottom, and center lines of all “happy” bunny-ear characters. Individual configurations and averages created from the k-means clustering analysis are overlaid.

- All ear lines (top, bottom, and center) were scaled to 10” long regardless of ear type (floppy or bunny).
- Lines were rotated to control for head orientation.
- Only left ears were traced unless these were partially obscured. If obscured, the right ear was traced and mirrored to the left side.

B. Analysis of Image Configuration

The image lines were analyzed using the “R” statistical environment to create an ideal configuration for each emotion. All ear configuration lines were composed of a series of 11 points (where “point zero” was at the origin) to match the configuration of our robot fin. Bunny and floppy ears were analyzed separately, as were the top, center, and bottom lines. Based on the resulting 2D density plots, the data were multimodal; thus, we conducted a k-means clustering analysis to create multiple averages for each emotion (Fig. 3). The k-means analysis was done by clustering different images lines together by the x or y location of individual points in the sequence. We compared the variance in the k-means analysis for points 6-11 only, as points 0-5 were all close to the origin and did not indicate much about the overall ear position. We found that, for bunny ears, the best grouping (lowest variance) was found for points 8 and 11; for floppy ears, it was points 9 and 10. Only the resulting center line averages (from these low variance points) that aligned with the density plots were selected and used for a validation study.

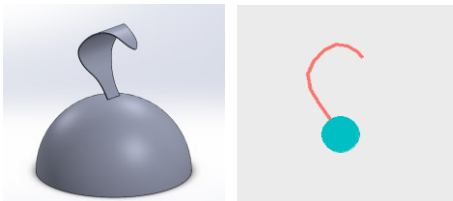


Figure 4. 3D visual (left) and its average line counterpart (right)

C. Validation of Image Configuration

To verify that our calculated averages conveyed the expected emotion, we conducted an online validation study with adults. The survey used two different representations of the averages: the first was the k-means average line with a


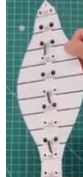






point at one end to provide orientation, and the second was a parametric SolidWorks model that showed a 3D view of the fin following the average line (Fig. 4). The images were presented to study participants so that all of the line visuals were shown before the 3D visuals; images were counterbalanced within these groups so that the additional information in the 3D models did not influence the perception of the more abstract line images. Participants were asked to classify each image as one of the Ekman emotions in the same way as our initial cartoon codifying. The survey was completed with 160 adults on *Prolific*, and a chi-squared “goodness of fit” analysis was conducted for all images. For the line images, 60 of the 75 images had significant agreement, but none of the agreed emotions matched with our “expected” emotions. Out of the 30 3D visuals, 29 had significant agreement and 11 of these matched our intended emotions. Table II shows the p-values and Cohen’s d-effects size for the significant, matched configurations. The agreed emotion configurations included four of the six Ekman emotions: anger, happiness, sadness, and surprise. There were no significant and matching configurations for fear or disgust.

TABLE II. SIGNIFICANT & EMOTION MATCHED CONFIGURATIONS

| Significant Results with Matched Anticipated & Perceived Emotion | | | | | |
|--|---------------|----------|---------|-----------|------------------------|
| Ear Type | k-means Point | χ^2 | P-Value | Cohen's d | Emotion |
| Bunny | 11 | 25.60 | <0.001 | 0.57 | Anger ^a |
| Bunny | 11 | 55.90 | <0.001 | 0.84 | Happiness ^a |
| Bunny | 11 | 12.70 | 0.0264 | 0.40 | Happiness |
| Bunny | 8 | 42.25 | <0.001 | 0.73 | Happiness |
| Bunny | 11 | 47.95 | <0.001 | 0.77 | Surprise |
| Bunny | 8 | 57.15 | <0.001 | 0.84 | Surprise ^a |
| Bunny | 11 | 139.51 | <0.001 | 1.33 | Sadness |
| Floppy | 10 | 18.40 | 0.0025 | 0.48 | Happiness |
| Floppy | 10 | 19.45 | 0.0016 | 0.49 | Surprise |
| Bunny | 8 | 152.05 | <0.001 | 1.38 | Sadness ^a |
| Floppy | 10 | 130.78 | <0.001 | 1.27 | Sadness |

^aUsed for final configuration design

TABLE III. INITIAL FIN TEST DESIGNS & RESULTS

| Test | Continuum HDPE | Continuum PS | Continuum Silicone | Kerf-equal | Kerf-unequal | Corrugated Plastic | Links | Links & Springs |
|------------------|---|---|---|---|---|---|---|---|
| Image |  |  |  |  |  |  |  |  |
| Load Test (3#) | Pass | Pass | Pass | Partial | Pass | Pass | Pass | Pass |
| Max. Pull Force | 1 lb 2 oz | - | 2lb 12 oz | 2lb 6oz | 5lbs | 12 oz | 10 oz | 3lbs 4 oz |
| Max. Joint Angle | 38° | 27° | 25° | 28° | 25° | 108° | 43° | 45° |
| Cycle Test | Pass | Full Fracture | Pass | Minimal | Minimal | Pass | Pass | Pass |
| Tear (0-2) | 1 | - | 0 | 2 | 2 | 1 | 0 | 0 |
| Twist (0-2) | 2 | - | 0 | 2 | 2 | 1 | 0 | 0 |
| Pull (0-2) | 0 | - | 0 | 1 | 0 | 0 | 0 | 0 |
| Fold (0-2) | 1 | - | 0 | 2 | 0 | 1 | 0 | 0 |

IV. PROTOTYPE TESTING

From our configurations, we sought to design a continuum robotic fin that could achieve the different required configurations at a relatively quick speed (1.0 seconds from rest to final position). This speed constraint was created to underscore the importance of dynamics in non-verbal communication: quicker movements could be slowed down in the final application.

A. Initial Fin Design & Testing

Our initial tests considered eight total designs: five different continuum designs and three variations of hyper-redundant designs. Table III shows all eight designs. Each design had no more than 10 connection points for the main tendon. The continuum designs included two designs made from 1/32" plastic (HDPE, PS), two made from a laser cut kerf bent sheet of 1/8" plywood (equal, unequal pattern spacing), and one made of 1/4" thick silicone. The hyper-redundant designs were corrugated plastic cut on one side at the joints, and two variations of a 3D-printed link-and-dowel system (with and without opposing side springs). With the exception of the linkage systems, all the designs had the same 12" long fin shape. Because the links were significantly heavier than the other designs, they were tested as a straight 1" wide spine of eight 1" long links.

Each fin design was then put through a variety of tests to compare mechanical properties. We conducted four mechanical tests: load bearing (3lbs), required pull force (maximum), maximum achievable joint angle (at max pull force), and deformation cycle (100 cycles) tests. We also conducted four damage tests: tear, twist, pull, and fold. Each of the damage tests were done by hand and scored on a 0 – 2 scale, where a score of "0" indicated no visible damage, a score of "1" indicated some visible damage, and a score of "2" indicated complete failure (no longer useable with the tendon) (see scoring in Table III).

Based off these tests, we decided to further pursue the 3D printed linkage design, the corrugated plastic design, and the silicone design. The silicone and link designs proved extremely durable: they had no damage from any test. The

corrugated plastic sustained some damage but had a very low pull force and high joint angle that made it an attractive alternative to the silicone and link designs. The other design options tested (kerf bent plywood, continuum plastics) sustained a degree of damage that could be problematic with the transport and interaction required for user studies.

B. Configuration Design Analysis

Each of the chosen designs was then fit to the robot base with a stepper motor for further testing. The corrugated and silicone fins were set to the actual fin shape (12" tall with 10 joints or attaching segments) while the linkages were tested as a narrow column of linkages. The testing setup consisted of a base to hold the fin in place and a 5V NEMA 11 stepper motor with a holding torque of 13 oz-in. Attached to the stepper motor was a pulley wheel with a 0.75" diameter. Testing consisted of running the stepper motor in quarter-turn intervals, from a quarter turn up to a full turn. This allowed us to assess the different shapes a specific fin setup was capable of making, and how the curvature would fit our desired configurations. Each of the three fin configurations could be set up with 1" extension springs to achieve different shapes. We used four springs ranging in stiffness from 0.77lbs/in to 5.44lbs/in. All tests used only one tendon that was attached at the end joint of the fin on the opposite side of the springs.

The focus of these tests was to determine which fin could achieve the qualitative characteristics of our animation configurations in a single setup (without changing the springs). The qualitative attributes we found among our significant and matched configurations were *straight up*, *straight with a high angle near the base*, *compound curves*, and *angles above 25 degrees*. While the links could achieve all of these shapes, each shape required different springs, and the pull force often stalled the motors. The silicone design achieved all of these shapes and only needed a different spring configuration for the compound curve. The corrugated plastic achieved all of the shapes except for the compound curve which was not possible with any spring setup.

While the silicone and the corrugated plastic designs could achieve the same qualitative characteristics in a single setup, the true continuum design of the silicone was more visually

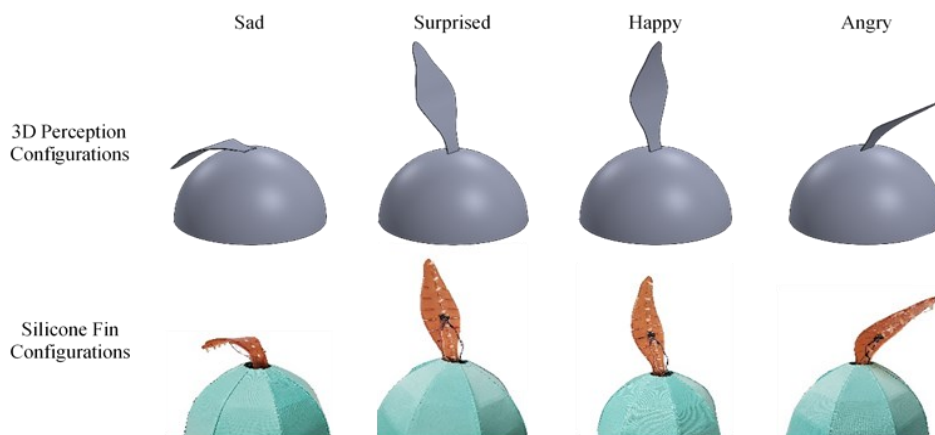


Figure 5. Final silicone fin configurations with their corresponding configuration

appealing than the rigid segments of the corrugated plastic design. Additionally, our initial tests showed the silicone to be more durable. Thus, our final configuration analysis focuses on the continuum silicone design.

C. Final Configuration & Setup

After initial testing and evaluation, the continuum silicone design was studied to achieve the emotion configurations from our validation study. For the emotions that had multiple configuration options in our validation study, we focused on the configuration with the highest effect size, making it the most likely to be correctly identified (refer to Table II).

To achieve these configurations, we tested six (of a possible eight) two-tendon setups. The tested setups allowed tendons to be fixed on either the front or back of the fin and at either the halfway point or the very end of the fin. Of the eight possible setups, two were not tested as they would not provide fin control along the entire length of the fin or they would not span more than 45 degrees-of-range of motion, based on the resting position of the fin (Table IV). Of the six tested setups, only one could achieve all four of the desired emotion configurations.

In the final setup, the silicone fin was fully fixed to the base, which limited the maximum joint angle that could be achieved near this point. For this reason, specific configurations were visually matched to the 3D configurations rather than calibrated to specific angles (Fig. 5). The final setup also includes a mounted gyro +

accelerometer which allowed the orientation of the center ‘link’ to be captured so that configurations can be based on orientation and not motor steps (minimizing slack error).

V. APPLICATION

We were able to use the continuum appendage to communicate four of the six core Ekman emotions: happiness, sadness, anger, and surprise. While we were unable to identify a static condition for fear, this may be because fear is often better expressed with gestures, such as turning away and retreating [9]. In our setup, fear may still be achievable, as the stepper motor on the base of the fin allows for rotation about the vertical axis (to create a motion of turning away and down, or just driving away from an object). Lastly, while these six core emotions represent only a small number of the range of emotions that cartoons (and people) express, they provide a good starting point for base configurations. From here, we can account for variations by changing speed and motion path around these static poses.

Given these achievable static emotions and their possible variations with the introduction of movement, our fin is capable of communicating the majority of emotions experienced by the cartoons referenced. For instance, we have demonstrated that our robot can convey the emotions of the character “Stitch” from Disney’s Lilo & Stitch. In the Disney movie, Stitch is initially an *angry*, chaos-creating alien who gets adopted by Lilo, a young girl. After causing all kinds of trouble for Lilo and her family, Stitch feels overwhelmingly *sad* and decides that the best thing to do is to leave them. Upon leaving, Stitch is *surprised* to find the aliens have been waiting for this moment to take him away from the family. At the end of the movie, Lilo saves Stitch from the aliens, which makes Stitch *happy* as he can rejoin Lilo’s family on Earth. Our current fin design could convey all four core emotions Stich exhibits in this popular children’s movie, suggesting that our robot has the capacity to convey the emotions of the popular animated characters it was designed from.

Future studies will look to validate how children perceive these fin positions, and how dynamics can be developed to improve this perception. We also consider the situations in which these affective displays will enhance children’s communication and interactions with the robot in cooperative tasks.

TABLE IV. TENDON SETUP TESTS

| Fin Type | Angry | Happy | Surprised | Sad |
|-----------------------|-------|-------|-----------|-----|
| ½ Front, ½ Back | N/A | N/A | N/A | N/A |
| ½ Front, Full Back | Yes | No | Yes | Yes |
| ½ Front, Full Front | Yes | Yes | Yes | Yes |
| Full Front, Full Back | No | Yes | Yes | No |
| Full Front, ½ Back | No | Yes | Yes | Yes |
| ½ Back, Full Back | N/A | N/A | N/A | N/A |
| Full Front - | No | Yes | Yes | No |

VI. CONCLUSION

Our cartoon analysis and validation study revealed that our continuum fin appendage may be able to communicate four of the six core Ekman emotions (happiness, sadness, anger, and surprise) in static configurations based on calculated average positions from a selection of cartoon bunny and floppy ears. Unlike previous work which focuses on animator designed or algorithmically generated emotions, we present a bottom-up method of affective configuration generation focused on extracting the knowledge of various animators from static cartoon images they generated. While our approach was functional for many emotions with the 3D representations of our averages, reducing the animation dimensionality to a single line did not lead to perceptions of the expected emotions. Thus, when using this approach, it is important that the robot design has similar dimensionality to the animated shape being studied; in our case, using a continuum antenna in our configurations may not have conveyed the intended emotion. Further, fear and disgust were not validated in our final analysis; this may be because disgust is underrepresented in these types of characters (we only had five images that we classified as such), and fear is often represented by the character retreating [9] which cannot be represented in a static configuration.

Further, we present a comparison of the mechanical properties of various tendon driven continuum robot designs. We considered different materials (plastic, plywood, silicone) and different types of systems (true continuum and hyper-redundant). We found that the continuum silicone design worked best for our application, being extremely durable and easy to actuate simply with two-tendons to achieve different shapes. In contrast, the designs in plastic were far less durable and susceptible to plastic deformation while the 3D-printed links were effective but required a much greater pull force to stand upright (often stalling our motors). Despite this, the 3D printed links are a very accessible option for continuum designs when not required to stand upright.

The research reported here offers a novel design and application of continuum and, more broadly, non-humanoid robots as effective conveyers of emotions—a necessary trait as robots become increasingly integral to our everyday lives.

REFERENCES

- [1] M. P. Michalowski, S. Sabanovic, and P. Michel, "Roillo: Creating a social robot for playrooms," *Proc. - IEEE Int. Work. Robot Hum. Interact. Commun.*, pp. 587–592, 2006.
- [2] L. Arnold, "Emobie™: A robot companion for children with anxiety," *ACM/IEEE Int. Conf. Human-Robot Interact.*, vol. 2016-April, pp. 413–414, 2016.
- [3] A. Ramachandran, C. M. Huang, E. Gartland, and B. Scassellati, "Thinking Aloud with a Tutoring Robot to Enhance Learning," in *ACM/IEEE International Conference on Human-Robot Interaction*, 2018.
- [4] P. Baxter, C. De Jong, R. Aarts, M. De Haas, and P. Vogt, "The effect of age on engagement in preschoolers' child-robot interactions," *ACM/IEEE Int. Conf. Human-Robot Interact.*, pp. 81–82, 2017.
- [5] J. Bates, "The Role of Emotion in Believable Agents," *Commun. ACM*, vol. 37, no. 7, pp. 122–125, 1994.
- [6] C. Parlitz, M. Hägele, P. Klein, J. Seifert, and K. Dautenhahn, "Care-

- o-bot 3 - Rationale for human-robot interaction design," *39th Int. Symp. Robot. ISR 2008*, no. November 2015, pp. 275–280, 2008.
- [7] J. Aronoff, B. A. Woike, and L. M. Hyman, "Which Are the Stimuli in Facial Displays of Anger and Happiness? Configurational Bases of Emotion Recognition," *J. Pers. Soc. Psychol.*, vol. 62, no. 6, pp. 1050–1066, 1992.
- [8] L. Anderson-Bashan *et al.*, "The Greeting Machine: An Abstract Robotic Object for Opening Encounters," *RO-MAN 2018 - 27th IEEE Int. Symp. Robot Hum. Interact. Commun.*, pp. 595–602, 2018.
- [9] F. Gerlinghaus, B. Pierce, T. Metzler, I. Jowers, K. Shea, and G. Cheng, "Design and emotional expressiveness of Gertie (An open hardware robotic desk lamp)," *Proc. - IEEE Int. Work. Robot Hum. Interact. Commun.*, pp. 1129–1134, 2012.
- [10] M. Bretan, G. Hoffman, and G. Weinberg, "Emotionally expressive dynamic physical behaviors in robots," *Int. J. Hum. Comput. Stud.*, vol. 78, pp. 1–16, 2015.
- [11] F. Manzi *et al.*, "A robot is not worth another: Exploring children's mental state attribution to different humanoid robots," *Front. Psychol.*, vol. 11, no. September, pp. 1–12, 2020.
- [12] C. L. van Straten, J. Peter, R. Kühne, and A. Barco, "Transparency about a robot's lack of human psychological capacities: Effects on child-robot perception and relationship formation," *ACM Trans. Human-Robot Interact.*, vol. 9, no. 2, 2020.
- [13] T. N. Beran and A. Ramirez-Serrano, "Do children perceive robots as alive?," p. 137, 2010.
- [14] D. Kocher, T. Kushnir, and K. E. Green, "Better together: Young children's tendencies to help a non-humanoid robot collaborator," *Proc. Interact. Des. Child. Conf. IDC 2020*, pp. 243–249, 2020.
- [15] J. J. Cabibhan, H. Javed, M. Ang, and S. M. Aljunied, "Why Robots? A Survey on the Roles and Benefits of Social Robots in the Therapy of Children with Autism," *Int. J. Soc. Robot.*, vol. 5, no. 4, pp. 593–618, 2013.
- [16] D. E. Logan *et al.*, "Social robots for hospitalized children," *Pediatrics*, vol. 144, no. 1, 2019.
- [17] J. Kennedy, P. Baxter, and T. Belpaeme, "The Robot Who Tried Too Hard: Social Behaviour of a Robot Tutor Can Negatively Affect Child Learning," *ACM/IEEE Int. Conf. Human-Robot Interact.*, vol. 2015-March, pp. 67–74, 2015.
- [18] C. L. Breazeal, *Designing Sociable Robots*. MIT Press, 2002.
- [19] M. S. Erden, "Emotional Postures for the Humanoid-Robot Nao," *Int. J. Soc. Robot.*, vol. 5, no. 4, pp. 441–456, 2013.
- [20] C. Zaga, R. A. J. De Vries, J. Li, K. P. Truong, and V. Evers, "A simple nod of the head: The effect of minimal robot movements on children's perception of a low-anthropomorphic robot," *Conf. Hum. Factors Comput. Syst. - Proc.*, vol. 2017-May, pp. 336–341, 2017.
- [21] M. Inderbitzin, A. Valjamae, J. M. B. Calvo, P. F. M. J. Verschuren, and U. Bernardet, "Expression of emotional states during locomotion based on canonical parameters," *2011 IEEE Int. Conf. Autom. Face Gesture Recognit. Work. FG 2011*, no. April, pp. 809–814, 2011.
- [22] D. Trivedi, C. D. Rahn, W. M. Kier, and I. D. Walker, "Soft robotics: Biological inspiration, state of the art, and future research," *Appl. Bionics Biomech.*, vol. 5, no. 3, pp. 99–117, 2008.
- [23] M. Wooten, C. Frazelle, I. D. Walker, A. Kapadia, and J. H. Lee, "Exploration and inspection with vine-inspired continuum robots," *Proc. - IEEE Int. Conf. Robot. Autom.*, pp. 5526–5533, 2018.
- [24] R. Sirohi, Y. Wang, S. Hollenberg, I. S. G. Keith, I. D. Walker, and K. E. Green, "Design and characterization of a novel, continuum-robot surface for the human environment," *IEEE Int. Conf. Autom. Sci. Eng.*, vol. 2019-Augus, pp. 1169–1174, 2019.
- [25] S. Chunduri, Y. Wang, I. D. Walker, and K. E. Green, "Design and Characterization of a Novel Continuum Robot Surface to Configure Physical Environments."
- [26] Y. Wang, C. Frazelle, R. Sirohi, L. Li, I. D. Walker, and K. E. Green, "Design and characterization of a novel robotic surface for application to compressed physical environments," *Proc. - IEEE Int. Conf. Robot. Autom.*, vol. 2019-May, pp. 102–108, 2019.